

NOTATION

a	= growth rate parameter
C_m	= metastable concentration
C_s	= solubility concentration
f_2	= dimensionless normalized second moment
f_2'	= dimensionless perturbed normalized second moment
$g(L), g(x)$	= size-dependent growth rate function
G	= growth rate
G_0^0	= steady state growth rate
i	= nucleation sensitivity parameter
L	= crystal size
L_1	= crystal size where growth rate changes
n	= population density
n_0	= steady state population density
n^0	= nuclei density
V	= crystallizer volume
x	= dimensionless crystal size = $L/G_0^0\tau$
x_1	= dimensionless crystal size = $L_1/G_0^0\tau$
$\bar{x}_{i,j}$	= dimensionless mean size as ratio of i 'th and j 'th dimensionless moments.
y	= dimensionless population density n/n^0
\bar{y}	= dimensionless steady state population density
y'	= dimensionless perturbed population density

Greek Letters

ϕ	= dimensionless growth rate = G^0/G_0^0
θ	= dimensionless time = t/τ
τ	= residence time, V/Q

LITERATURE CITED

1. Anshus, B. E. and E. Ruckenstein, "On the stability of a well stirred isothermal crystallizer," *Chem. Eng. Sci.*, **28**, 501 (1973).
2. Garside, J. and S. J. Jancic, "Growth and dissolution of potash alum crystals in the subsieve size range," *AIChE J.*, **22**, 887 (1976).
3. Randolph, A. D., "CSD dynamics, stability, and control," in CEP Symposium Series, *Design control and analysis of crystallization processes*, (in press).
4. Randolph, A. D., Beer, G. L. and J. P. Keener, "Stability of the class II classified product crystallizer with fines removal," *AIChE J.*, **19**, 1140 (1973).
5. Randolph, A. D., and M. A. Larson, *Theory of particulate processes*, p. 231, Academic Press, New York (1971).
6. Randolph, A. D. and S. K. Sikdar, "Creation and survival of secondary crystal nuclei. The potassium sulfate—water system," *Ind. Eng. Chem. Fundam.*, **15**, 64 (1976).
7. Sherwin, M. B., Shinnar, R. and S. Katz, "Dynamic behavior of the well-mixed isothermal crystallizer," *AIChE J.*, **13**, 1141 (1967).
8. Sherwin, M. B., Shinnar, R. and S. Katz, "Dynamic behavior of the isothermal well-stirred crystallizer with classified outlet," C.E.P. Symp. Ser., **65**, (95), 75 (1969).

Manuscript received August 7, 1978; revision received June 8, and accepted July 11, 1979.

On the Concentration Dependence of Diffusion Coefficients in Zeolites

D. GELBIN and K. FIEDLER

Central Institute of Physical Chemistry
Academy of Sciences of German Democratic Republic
Berlin, GDR

Ruthven (1976) published thermodynamic and kinetic data on the adsorption of five gases in zeolites over a wide range of temperatures and concentrations. We have described zeolite diffusivities with a model based on the discrete structure of zeolite crystals and a statistic-thermodynamic evaluation of equilibrium measurements (Fiedler and Gelbin 1978). Prof. Ruthven has kindly sent us tables of results for all systems in his paper, which we analyze below.

THE MODEL DESCRIBED

According to statistical thermodynamics, adsorption equilibrium may be calculated as

$$\theta_a = \frac{a}{N_c} = \sum_{i=1}^m i \theta_i \quad (1)$$

$$\theta_i = \frac{\left(\frac{P/P_0}{T/T_0}\right)^i \exp [i (S_i T - E_i)/RT]}{1 + \sum_{j=1}^m \left(\frac{P/P_0}{T/T_0}\right)^j \exp [j (S_j T - E_j)/RT]} \quad (2)$$

By curve-fitting equilibrium isotherms at several temperatures, the N_c , E_i and S_i may be determined and used to calculate the θ_i . A distribution of cages holding different numbers of molecules at any average condition is commonly observed. We therefore describe molecular transport between cages by the equation

$$\theta_i p_i + \theta_{j-1} = \theta_{i-1} + \theta_j p_j \quad (3)$$

Equation (3) states that a mobile molecule jumps from a cage holding i molecules to one holding $j-1$ molecules, leaving a cage holding $i-1$ molecules and one holding j molecules, one of which is mobile. Local equilibrium between mobile and localized molecules is established immediately. The possibility of more than one molecule in a cage being mobile at any instant is neglected.

Using standard methods and straightforward mathematics we derive

$$D_z = \frac{\sum_{i=1}^m D_{i,i-1} p_i \theta_i \theta_{i-1} + 2 \sum_{i=2}^m \sum_{j=1}^{i-1} D_{i,j-1} p_i \theta_i \theta_{j-1}}{\sum_{i=1}^m i (i - \theta_a) \theta_i} \quad (4)$$

where

$$\frac{\partial \theta_a}{\partial (\mu/RT)} = \sum_{i=1}^m i (i - \theta_a) \theta_i \quad (5)$$

D_z is the diffusion coefficient determined from adsorption uptake experiments using Fick's law. The $D_{i,j-1}$ are the diffusivities according to Equation (3), and may vary with the number of molecules per cage. The $D_{i,j-1}$ are defined as the jump rate multiplied by the squared distance between adjacent cages. The product $\theta_i \theta_{j-1}$ is the probability that a cage holding i molecules has a neighbor holding $j-1$ molecules.

To derive Darken's law from Equation (4) we must make two assumptions:

1. The mobility of all molecules is equal, so that the jump rate is proportional to the number of molecules per cage. For $j = i$,

$$D_{i,i-1} p_i = i D_{x,x-1} p_x \quad (6)$$

The general expression for $j \neq i$ has been shown (Fiedler and Gelbin, 1978) to be

$$D_{i,j-1} p_i = \frac{1}{2} D_{x,x-1} p_x \left(i + j \frac{\theta_j \theta_{i-1}}{\theta_i \theta_{j-1}} \right) \quad (7)$$

In this case, $D_{x,x-1} p_x$ is the self-diffusivity and $\theta_j \theta_{i-1} / \theta_i \theta_{j-1}$ is an equilibrium constant.

Combining Equations (4, 5, 6, 7),

$$D_z = D_{x,x-1} p_x (1 - \theta_m) \frac{\partial(\mu/RT)}{\partial(\ln \theta_a)} \quad (8)$$

2. The second assumption is that all cages are permeable, so that cages occupied by m molecules permit passage of an additional molecule. The upper summation limits are raised from m to $m+1$, and the Factor $(1 - \theta_m)$ drops out of equation (8), which becomes identical with the Darken equation. Darken's law predicts that D_z becomes infinite at saturation; the term $(1 - \theta_m)$ reduces D_z to $m D_{x,x-1} p_x$ at saturation.

On the other hand, if molecule-to-molecule interference is large, the jump rate between cages could be independent of the number of molecules per cage.

For $j = i$

$$D_{i,i-1} p_i = D_{x,x-1} p_x \quad (9)$$

and for $j \neq i$

$$D_{i,j-1} p_i = \frac{1}{2} D_{x,x-1} p_x \left(1 + \frac{\theta_j \theta_{i-1}}{\theta_i \theta_{j-1}} \right) \quad (10)$$

Equations (4) and (5) now simplify to

$$D_z = D_{x,x-1} p_x \frac{1 - \theta_0}{\theta_a} (1 - \theta_m) \cdot \frac{\partial(\mu/RT)}{\partial(\ln \theta_a)} \quad (11)$$

If, at intermediate coverages $\theta_0 \ll 1$ and $\theta_m \ll 1$, Equation (11) reduces to the model of Ruthven (1976), in which Darken's diffusivity is inversely proportional to θ_a .

The curves were fitted by a standard least-squares deviation program using an iterative Newton procedure, with optional restrictions on the parameters. It was possible to set values equal at two occupation levels if data were insufficient for discrimination. In Table 1, several cases may be recognised where this option was taken. Parameters were determined isothermally for the kinetic curves, but preferably overall temperatures for the equilibrium curves.

THE THERMODYNAMIC RESULTS

The thermodynamic data determined by Equations (1) and (2) for three of the five systems are presented in Table 1. The fractional number of cages per unit weight N_c relative to the theoretical number fluctuates about unity. The adsorption entropy S_i decreases with rising occupation level for *n*-heptane in both zeolites, but remains constant for toluene in 13X. This correlates with the increasing loss of configurational degrees of freedom when the long-chained paraffin is adsorbed, whereas only minor distortion of the more rigid toluene molecule is possible. The high entropy losses for toluene in 13X correspond to the low available free volume within the cage. It was our experience in analyzing equilibrium data that the adsorption energy E_i tends to be only weakly dependent on the number of

TABLE 1. THERMODYNAMIC DATA

System	N_c	i	$-S_i$	$-E_i$
	$N_{c, theo}$			
<i>n</i> -heptane/13X	0.873	1	44.7	48 200
		2	80.7	64 500
		3	87.4	64 000
toluene/13X	1.10	1	127.6	93 300
		2	116.2	84 100
		3	129.3	85 700
<i>n</i> -heptane/5A	0.95	1	89.9	72 800
		2	105.2	76 100
		3	125.9	76 100

molecules per cage. We do not attach any physical significance to the low energy value of the first *n*-heptane molecule in 13X. All other adsorption energies are about equal in a given system.

In curve-fitting the equilibrium data for cyclohexane and benzene in NaX, the optimum number of cavities N_c tended to drop to only two-thirds of the theoretical number. Since the experiments were not performed in our laboratories, we are not in a position to determine the reasons for this deviation from expected performance. We chose to fit the equilibrium curves isothermally at each temperature, so that adsorption energies and entropies are not available in these two systems.

THE KINETIC RESULTS

In fitting Equation (4) to the rate data in the 13X zeolite, the diffusivities in the second summation of the numerator were of no statistical significance. These terms were therefore neglected and the parameter search restricted to the $D_{i,i-1} p_i$. For *n*-heptane/13X, $D_{i,i-1} p_i$ is independent of the number of molecules per cage, and values at all occupation levels cluster around a common Arrhenius line, Figure 1, Curve 1. The activation energy of 5.6 kcal/mole agrees well with that of 6.2 kcal/mole found by Ruthven (1976). For toluene the diffusivities increase with molecular loading, Figure 1, Curves 2-4. The activation energies are 11.7, 8.5 and 3.4 kcal/mole with increasing occupation level, compared to the 5.6 kcal/mole of Ruthven (1976).

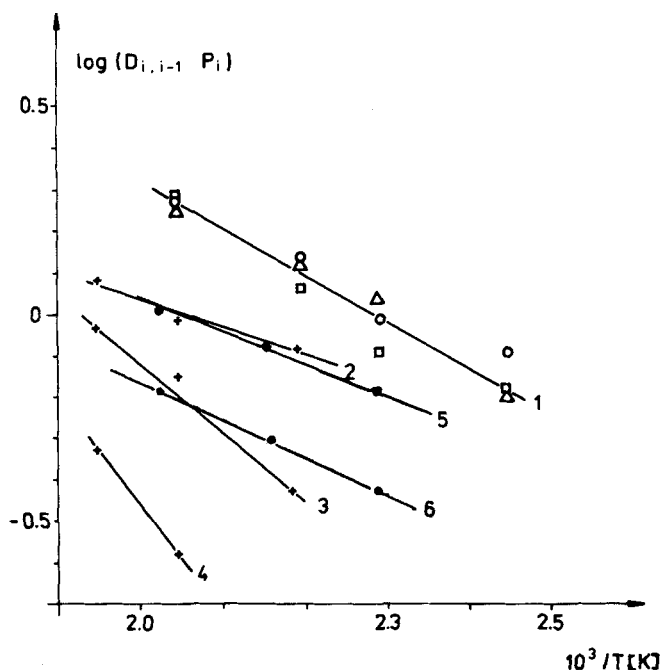


Figure 1. Cage diffusivity vs. reciprocal temperature 1. *n*-heptane/13X, all occupation levels; 2. toluene/13X, $D_{32} p_3$; 3. ditto, $D_{21} p_2$; 4. ditto, $D_{10} p_1$; 5. *n*-heptane/5A, $D_{x,x-1} p_x$, Eqn. 11; 6. ditto, Eqn. 8. Curves 1-4 in $\log(10^{-8} \text{ cm}^2 \text{ s}^{-1})$, Curves 5-6 in $\log(10^{-10} \text{ cm}^2 \text{ s}^{-1})$.

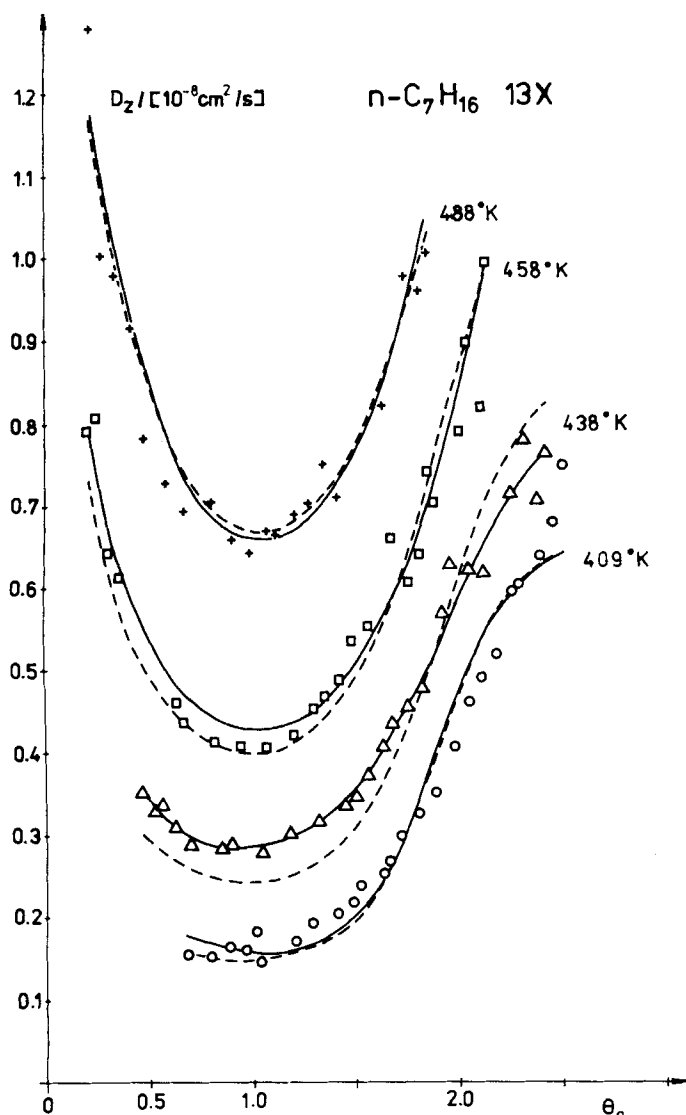


Figure 2. Effective diffusivity vs. loading for *n*-heptane/13X; — Equation (4), individual $D_{i,j-1} p_i$; --- Equation (4), constant average $D_{i,j-1} p_i$.

The best fit calculations of D_z as a function of the adsorbate concentration are shown for *n*-heptane/13X in Figure 2. The solid lines were calculated using equation (4) with the individual $D_{i,j-1} p_i$ from Figure 1; for the dashed lines, a constant average value was used at each temperature. Our equation predicts the minimum D_z at intermediate concentrations despite the constant $D_{i,j-1} p_i$. The comparison between experimental values and those calculated using Equation (4) and the diffusivities of Figure 1 for toluene/13X is equally good (Figure 3). The standard deviation of the calculated from the observed values is in all cases of the order of 1%.

The derivation of Equations (8) and (11) includes Equations (7) and (10) to describe the behavior of the $D_{i,j-1} p_i$, $i > j$. Using Equation (8) for toluene/13X or Equation (11) for *n*-heptane/13X, standard deviation increased to a level of 10-25%, and agreement was poor over the entire concentration range. With Equation (4) the $D_{i,j-1} p_i$, $i > j$, could not be determined satisfactorily by curve fitting. The results of all three Equations (4, 8, 11) indicate that jumps between cages differing in occupation level by two or more molecules do not contribute to flux in the 13X zeolite appreciably.

The diffusivities in the cyclohexane and benzene systems, (Table 2) show considerable scatter, which may be due to experimental inaccuracies, either in the thermodynamic or kinetic data, or both. Note that the experiments were not carried out

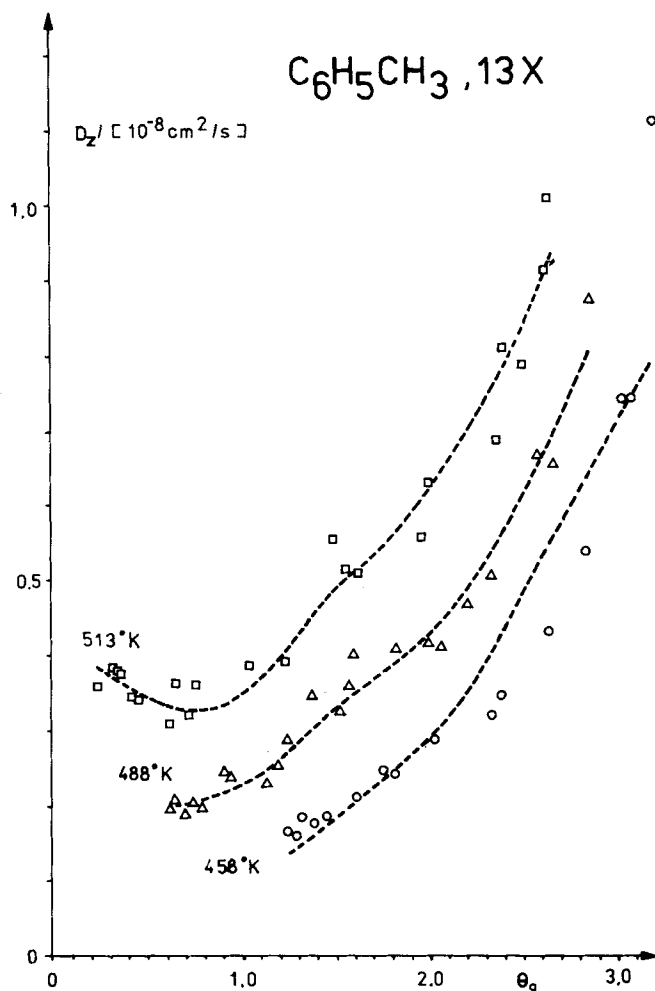


Figure 3. Effective diffusivity vs. loading for toluene/13X; --- Equation (4), individual $D_{i,j-1} p_i$.

TABLE 2. DIFFUSIVITIES IN NaX ($10^8 D_{i,j-1}$)

	<i>i</i>	409 K	437 K	458 K	488 K	513 K
cyclohexane	1	1.29	1.33	2.68	3.16	—
	2	1.48	2.30	1.92	3.05	—
	3	1.05	1.19	1.59	2.29	—
benzene	1	—	—	0.29	0.66	1.02
	2	—	0.63	0.88	1.09	1.67
	3	—	0.40	0.75	1.25	1.48
	4	—	0.78	0.98	1.24	1.75

with a view towards evaluation with our equations, and rechecking measurements as a result of parameter fluctuations, a common research procedure, was not possible under the prevailing conditions. But there does seem to be a tendency in Table 2 for the diffusivities to increase at low occupation levels for benzene, as well as for cyclohexane at the two lower temperatures. At higher occupation levels, diffusivities fluctuate about an average value or even decrease.

The data for *n*-heptane/5A lie within too narrow a range of concentrations to permit discrimination between the possible modes of behavior. Coverage varies from 0.3 to 1.5 molecules per cage at 491 K and from 0.7 to 1.7 molecules per cage at 439 K, whereas three molecules fit into a cage (Table 1). Curve fitting was performed satisfactorily with both Equations (8) and (11). In Figure 4, Equation (11) has been plotted at only one temperature but is equally good at all four. Large differences are to be expected only at higher concentrations, where θ_a becomes appreciable. The activation energy according to Equation (8) is 4.7 kcal/mole, according to Equation (11) 3.1 kcal/mole (Figure 1, Curves 5 and 6).

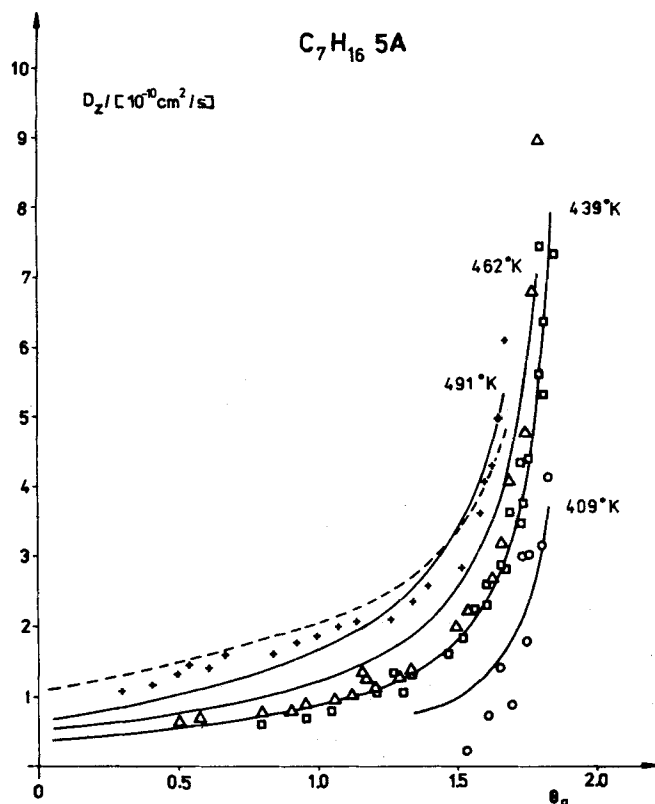


Figure 4. Effective diffusivity vs. loading for *n*-heptane/5A; — Equation (8), --- Equation (11).

DISCUSSION OF RESULTS

Our diffusivities are defined as the jump rate per cage multiplied by the squared distance between cages. The model may be interpreted as one in which cages of given occupation levels and not individual adsorbate molecules are moving downstream. The "cage diffusivity" or jump-rate per cage is related to the self-diffusivity of the adsorbate molecules, according to Equation (6). Jump rates increase with occupation level for toluene in 13X, so that adsorbate-adsorbate intermolecular disturbances are unimportant. The jump rate remains constant for *n*-heptane in 13X, so that adsorbate-adsorbate interaction is rate limiting. This agrees with the conception that adsorbed paraffin molecules are in a coiled configuration which does not fit through the window. The probability of a molecule stretching could decrease with increased loading.

Allowing for experimental error, benzene and cyclohexane behave as toluene at low loading levels, cage-molecule interaction appearing rate-limiting, whereas closer to saturation mobility is limited by intermolecular disturbance, as with *n*-heptane. Jump rates continue to increase in the toluene sys-

tem at higher loading rates than for benzene and cyclohexane, indicating relatively stronger adsorbate-lattice interaction for the alkylated ring compound.

Converting from cage diffusivities to self-diffusivities in the NaX-zeolites according to Equation (6), the self-diffusivity of toluene is independent of concentration, whereas that of *n*-heptane decreases proportional to occupation level.

Further, in the 13X studies no rate contribution has been found from jumps between cavities differing in occupation level by more than one. There is no evident reason why the $D_{i,j-1}p_i$ should be negligible. However, the $\theta_i\theta_{i-1}$, $i > j$ have been taken as the probability that a cage holding i molecules has a neighbor holding $j-1$ molecules; the θ_i are equilibrium values. The probability might be negligible during the kinetic experiment, if occupation levels were to advance in waves of cages holding one more (or less) molecule than the preceding wave. The final stage of the kinetic period would be internal rearrangement leading to the equilibrium distribution of occupation levels. Internal rearrangement does not appear to be a factor among the small-windowed 5A cages, since Equations (8) and (11) were applied successfully.

In this manner, our model Equation (4), which includes Darden's law (Equation 8) and the Ruthven model (Equation 11) as special cases, may be used to analyse adsorption rate behavior in zeolites.

NOTATION

a	= sorbate concentration, mol g ⁻¹
$D_{i,j-1}$	= diffusion coefficient, cm ² s ⁻¹
D_z	= Fickian diffusion coefficient, cm ² s ⁻¹
E_i	= energy of adsorption, J mol ⁻¹
m	= maximum no. of molecules per cage
N_c	= total number of cavities, mol g ⁻¹
P	= gas pressure, Pa
P_0	= standard pressure, Pa
p_i	= probability of motion
R	= gas constant, J K ⁻¹ mol ⁻¹
S_i	= standard entropy, J K ⁻¹ mol ⁻¹
T	= temperature, K
T_0	= standard temperature, K
θ_a	= reduced sorbate concentration
θ_i	= fraction of cavities holding i molecules
μ	= standard chemical potential, J mol ⁻¹

LITERATURE CITED

- Fiedler, K. and D. Gelbin, "Model for Analysing Diffusion in Zeolite Crystals," *J. C. S. Faraday Trans. 1*, **10**, 2423 (1978).
 Ruthven, D. M. and I. H. Doetsch, "Diffusion of Hydrocarbons in 13X Zeolite," *AIChE J.*, **22**, 882 (1976).

Manuscript received January 2, 1979; revision received July 12, and accepted July 23, 1979.

Approximate Formulae for the Dispersion Coefficients of Layered Porous Media

PEDER A. TYVAND

Department of Mechanics
 University of Oslo
 Oslo, Norway

Groundwater and petroleum reservoirs are composed of porous rocks. Very often these rocks constitute a layered structure.

Dispersion in porous media is very important in connection with groundwater pollution (Fried 1975) and oil production by secondary recovery (Pfannkuch 1963, Fried & Combarous 1971). Dispersion in layered porous media, represented as anisotropic in the macroscopic description, is determined by six dispersion